When Recovery Becomes Infeasible: A Markov Model of Housing Abandonment Risk in Flood-Prone Areas - Supplementary Material

Riccardo Negri[1], Susu Xu[2], Cristina-Ioana Dragomir[3], Inês Figueira[4], Maurizio Porfiri[5], and Luis Ceferino[6]

[1]PhD Candidate in Urban Systems, Department of Civil and Urban Engineering, New York University Tandon School of Engineering; Visiting PhD student, Department of Civil and Environmental Engineering, University of California, Berkeley. Email: r.negri@nyu.edu

[2]Assistant Professor, Department of Civil and Systems Engineering, Johns Hopkins University

[3]Clinical Associate Professor, Department of Liberal Studies, New York University; Technology Management and Innovation, New York University Tandon School of Engineering

[4]PhD Candidate in Mechanical Engineering, Department of Mechanical and Aerospace Engineering, New York University Tandon School of Engineering

[5]Institute Professor, Center for Urban Science and Progress, Department of Mechanical and Aerospace Engineering, Department of Biomedical Engineering, Department of Civil and Urban Engineering, New York University Tandon School of Engineering

[6]Assistant Professor, Department of Civil and Environmental Engineering, University of California, Berkeley

ZILLOW LISTING DATA

To calculate ψ_0 in each of the two case-study areas, we manually collected data from Zillow (August 2025) for a small sample of single-family houses (Tables S-1 and S-2). We restricted the sample to properties that appeared recently renovated or showed no visible need for repairs, based on listing photos. For active listings, we used the list price, while for off-market properties, we used Zillow's automated estimate of a home's market value based on publicly available data and

TABLE S-1. Sample of houses in good physical condition used to estimate the market price per square foot in Pascagoula, MS. The unit price is computed as the Zillow price (list price or Zestimate) divided by the reported interior floor area.

Address	**Unit price [USD/ft^2]**
2708 Canty St, Pascagoula, MS 39567	130.1
1815 Cherubusco St, Pascagoula, MS 39567	133.8
1807 Cherubusco St, Pascagoula, MS 39567	141.7
807 Columbus Dr, Pascagoula, MS 39567	133.7
811 Columbus Dr, Pascagoula, MS 39567	103.5
2621 Canty St, Pascagoula, MS 39567	155.8
611 Herrick Ave, Pascagoula, MS 39567	143.3
Average	134.5

TABLE S-2. Sample of houses in good physical condition used to estimate the market price per square foot in McGregor (Fort Myers, FL). The unit price is computed as the Zillow price (list price or Zestimate) divided by the reported interior floor area.

Address	**Unit price [USD/ft^2]**
522 Sanford Dr, Fort Myers, FL 33919	219.2
544 Bayside DR, FORT MYERS, FL 33919	241.8
5692 Eichen Cir W, Fort Myers, FL 33919	283.2
8746 Banyan Cove Cir, Fort Myers, FL 33919	247.4
5654 Natoma Dr, Fort Myers, FL 33919	192.4
5664 Natoma Dr, Fort Myers, FL 33919	248.5
1012 Wyomi Dr, Fort Myers, FL 33919	325.5
Average	251.1

recent sales of comparable properties (Zestimate). For each house, we computed the unit price as the total price in USD divided by the interior floor area in square feet, and then averaged the unit prices across the sample. To account for the possibility that asking prices may exceed final sale prices, we adopted slightly conservative values in our analysis: 130 USD/sqft instead of 134.5 for Pascagoula, and 240 USD/sqft instead of 251.1 for McGregor.

MODEL PARAMETERS ESTIMATION

We estimated the key parameters of our model using empirical data and findings from the literature. Our estimates are based on publicly available data from New York City following Hurricane Sandy, as well as previous scientific studies of other comparable flood events.

Price Drop After a Flooding

To estimate the relative drop in base price after a flood event (σ) and the time it takes for this discount to fade (τ_0), we relied on findings from empirical studies. Bin and Polasky (2004) found that properties in the floodplain of Pitt County, North Carolina experienced an increase in price discount after Hurricane Floyd (1999). Houses within the flood-prone area were already trading at a 3.8% discount relative to similar houses just outside the floodplain before the event. After the hurricane, the discount increased to 7.7%, a net increase of almost 4%. Ortega and Taşpınar (2018), studying Hurricane Sandy's impact in New York City, observed that undamaged properties in flood zones experienced an 8% price penalty, which persisted through 2017. Bin and Landry (2013), using data from the same region as Bin and Polasky, detected a 5.7% discount after Hurricane Fran (1996), which increased to 8.8% after Hurricane Floyd. They also found that these price discounts disappeared within 5 to 6 years. Similarly, Atreya et al. (2013) reported that flood-related price discounts faded between four and nine years after a major flooding event in Georgia. Based on these findings, we adopted $\sigma = 0.08$ (8% price drop) and $\tau_0 = 6$ years as our estimates.

Repair Rate

To estimate r, we analyzed construction permits issued in New York City after Hurricane Sandy. We focused on single-family houses that experienced at least 60 cm of floodwater during the storm. We estimated the flood depth at each house using the publicly available NYC Building Elevation and Subgrade (BES) dataset, which provides the first floor elevation (FFE) for every building in the city. We overlaid this dataset with the official map of Hurricane Sandy's inundation extent. Assuming a horizontal water profile (bathtub approach), we estimated water depth by subtracting each building's FFE from the ground elevation at the flood boundary. We excluded houses that changed building class after the hurricane (e.g., from single-family to multi-family), as these likely represent redevelopment rather than repair. We then selected houses that had at least one construction permit filed between the date of Hurricane Sandy and 2019. We applied this cutoff to exclude permits that occurred long after the event, and therefore are likely unrelated to flood damage. The final sample included 295 houses. From this sample, we calculated three metrics: the time between the start of the first permit and the end of the latest permit (Figure S-1a); the time between Hurricane Sandy (October 29, 2012) and the filing of the first permit (Figure S-1b); the time between Hurricane Sandy and the completion of the latest permit (Figure S-1c). The mean time between Hurricane Sandy and the conclusion of the latest permit was 5.4 years. Based on this, we assumed a value of r equal to 1/5 (0.20).

This analysis has several limitations. First, we cannot confirm that all construction permits in the sample were directly related to flood damage. Second, some households may have completed repairs without filing permits. Third, the timing of repairs depends on the availability of government aid and insurance payouts. If funding is disbursed earlier or later in other contexts, the average repair rate may differ. Fourth, the average repair time likely varies with the severity of the flood event. A large-scale disaster like Hurricane Sandy causes widespread damage, which can delay recovery by limiting access to contractors and construction resources. Nonetheless, our sensitivity analysis shows that the model is not highly sensitive to the choice of r, and our main conclusions remain robust despite these limitations.

NUMERICAL SOLUTION

We solve Equation 13 from the main article numerically to calculate the sub-replacement probability $\pi^{\text{sub}}(N)$, i.e., the probability that the house enters the sub-replacement set A at least once within a horizon of N years, starting from the initial state $(\psi^{(0)}, \delta^{(0)}, \tau^{(0)}) = (\psi_0, 0, \tau_0)$. To compute $\pi^{\text{sub}}(N)$ numerically, we first discretize the state space and approximate the continuous kernel K with a finite transition probability matrix (TPM). To do so, we discretize δ over its interval $[0, \delta_{\max}]$ and use $f_\delta^*(d)$ to estimate the probability mass associated with each discrete value. Second, we set a floor level for ψ. This floor can be chosen to be small enough so that further decreases in ψ would not affect the results (e.g., $\psi_{\text{floor}} = 0.01 \cdot \psi_0$). When ψ reaches ψ_{floor}, additional flooding no longer reduces ψ. Lastly, we cap τ at τ_0, meaning that when $\tau^{(n)}$ reaches τ_0, it stops increasing and remains there until the next flood occurs. With these three modifications,

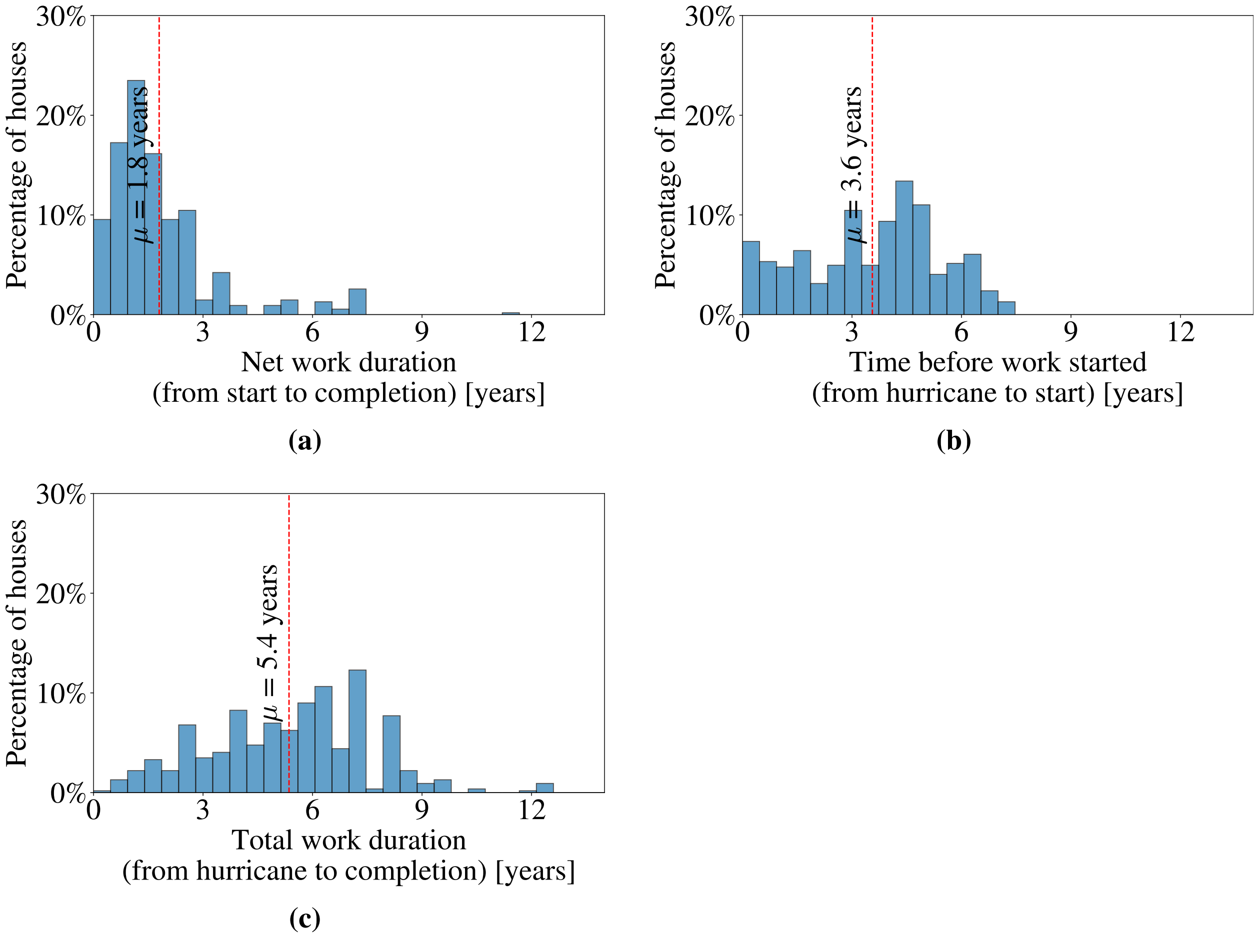

Fig. S-1. Construction permits for single-family houses in New York City that experienced at least 60 cm of flooding relative to the first floor elevation (FFE) during Hurricane Sandy. (a) Distribution of the time between the start and completion of permitted work. (b) Time elapsed between Hurricane Sandy (October 29, 2012) and the submission of the first permit. (c) Total duration of work measured from November 2012 to the completion of the last permit. The red dashed line indicates the mean value for each metric.

the state space $\{\psi\} \times \{\delta\} \times \{0, \ldots, \tau_0 - 1\}$ becomes finite.

We then arrange the discrete state space so that all non-sub-replacement states $S_T = \{(\psi, \delta, \tau) : \delta \leq \psi\}$ come first, and all sub-replacement states $S_A = \{(\psi, \delta, \tau) : \delta > \psi\}$ come last. From the discrete TPM, we extract the sub-matrix $Q \in \mathbb{R}^{|S_T| \times |S_T|}$, which contains transitions that remain within the non-sub-replacement region. To compute the survival probability (Equation 11 in the main manuscript), we introduce the row unit vector $\mathbf{e}_{i_0} \in \mathbb{R}^{1 \times |S_T|}$, which places probability equal to 1 on the initial state $(\psi_0, 0, \tau_0)$ and zero on all the other states. The survival probability is therefore given by

$$F_{\text{sub}}(N) = \mathbf{e}_{i_0}\, Q^N\, \mathbf{1}_T, \tag{S-1}$$

where $\mathbf{1}_T$ is the all-ones vector of length $|S_T|$. Equation (S-1) gives the survival probability of the system at step N, i.e. the total probability mass that the system has never entered the sub-replacement set A by step N. Finally, we can calculate the sub-replacement probability $\pi^{\text{sub}}(N)$ using Equation 12 of the main article.

On a workstation equipped with an 11th Gen Intel(R) Core(TM) i7-11700 CPU (2.50 GHz) and 64 GB of RAM, computing the 30-year absorption probability using the numerical method described above required, on average, about 0.03 seconds per house. For comparison, on the same hardware, estimating the same probability via Monte Carlo simulation with 10^6 runs per house—achieving a 95% confidence interval with a total width of approximately 10^{-3}—required about 18 seconds per house.

RISK ANALYSIS AT BLOCK-LEVEL

In the analysis reported in our main article, we assigned the same FFHAG to all houses in both communities (45 cm, approximately three stair steps). This simplification was necessary due to the lack of accurate FFHAG data at the house level for the full housing stock. In reality, FFHAG can vary substantially across properties. For example, visual inspection via Google Street View reveals that some homes in both Pascagoula and McGregor appear to be elevated by an entire floor (FFHAG $\geq$ 240 cm). These homes therefore face lower risk than previously estimated, both in terms of AAL and in terms of sub-replacement probability. Here, instead, we want to provide more realistic estimates of sub-replacement risk for a smaller sample of homes, where FFHAG can be manually estimated.

We focus on four houses in Pascagoula that, while subject to high flood exposure, do not appear elevated (Figure S-2a). Using Google Street View, we first estimate their FFHAG values and then rerun our model to compute updated AAL and sub-replacement probabilities. Figure S-3 shows our results. All four Pascagoula homes exhibit a 2–3.7% chance of entering sub-replacement within the next decade.

These probabilities increase approximately linearly with time over a five-decade period (Figure S-3a). This nearly linear trend arises from a characteristic of the model: the probability of entering A at every step (conditional on survival until the step before) remains nearly constant and is small relative to one. As a result, the survival probability decreases roughly linearly over the considered time horizon. By year 50, sub-replacement probabilities reach nearly 20%. However, projections over such long periods are less reliable, as they rely on the assumption of constant climatic and economic conditions. Over 50 years, other factors unrelated to flooding—such as demographic or economic shifts—may substantially alter housing demand in Pascagoula. For instance, the arrival of a major employer could raise incomes and drive up housing demand and prices, increasing ψ_0 independently of flood events. In addition, climate-related factors——such as sea level rise and changes in storm intensity——may significantly alter future flood hazard.

We also compare the four houses in Pascagoula with four houses in McGregor that face similar flood risk (Figure S-2b). These homes are among the most exposed in their community and have not been elevated. For both groups, we compare the AAL and the probability of entering sub-replacement within the next 30 years. Figure S-4 shows the results. AAL values remain higher for the McGregor homes, although they are within the same order of magnitude as those in Pascagoula. In contrast, the probability of entering sub-replacement diverges sharply. In Pascagoula, the probabilities are around 10^{-1}, while in McGregor they are closer to 10^{-4}—a difference of three orders of magnitude. For example, the most at-risk house in Pascagoula (Pas-1, Figure S-2) has an 11% chance of entering sub-replacement within the next 30 years, compared to just 0.02% for the most at-risk house in McGregor (McG-2). On the other hand, the house in McGregor has an AAL of nearly \$9,000, while the Pascagoula house has an AAL of about \$3,000. This comparison underscores once again how relying solely on AAL to measure flood risk can obscure important factors that could lead to housing abandonment.

SENSITIVITY ANALYSIS

We assess the sensitivity of our model to its key parameters: the yearly repair rate r, the

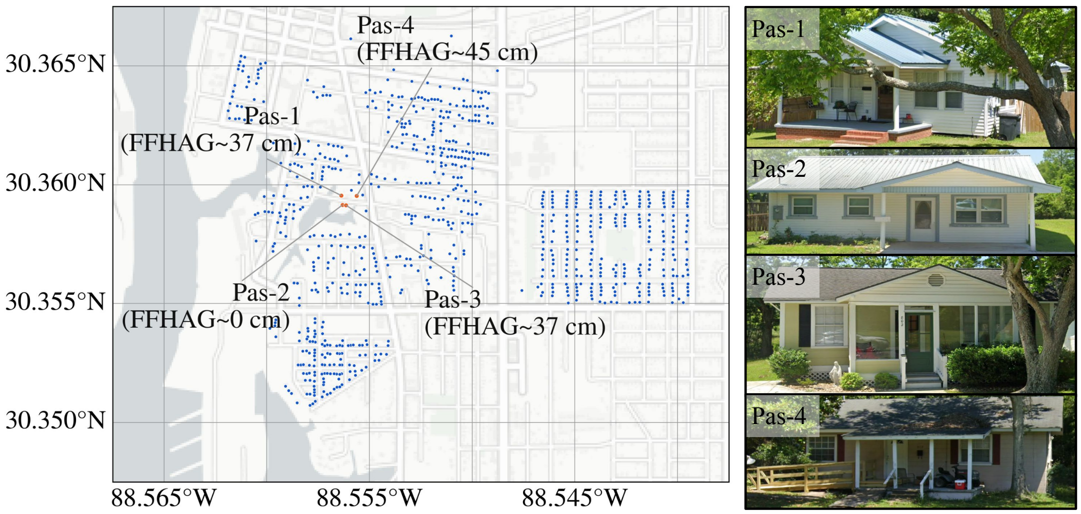

(a) Pascagoula, MS

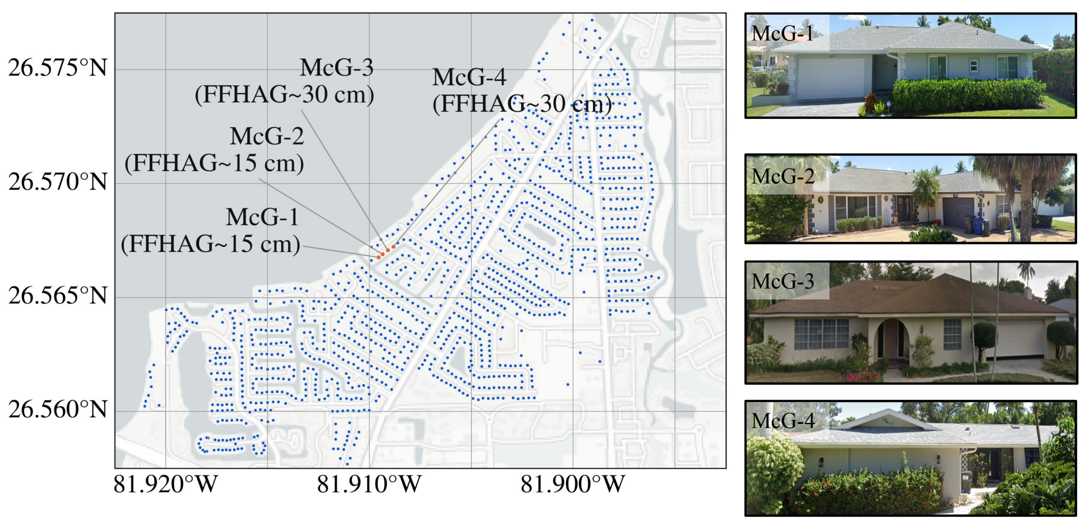

(b) McGregor, FL

Fig. S-2. Selected houses in Pascagoula (a) and in McGregor (b). FFHAG values are estimated based on Google Street View images, assuming each step is approximately 15 cm.

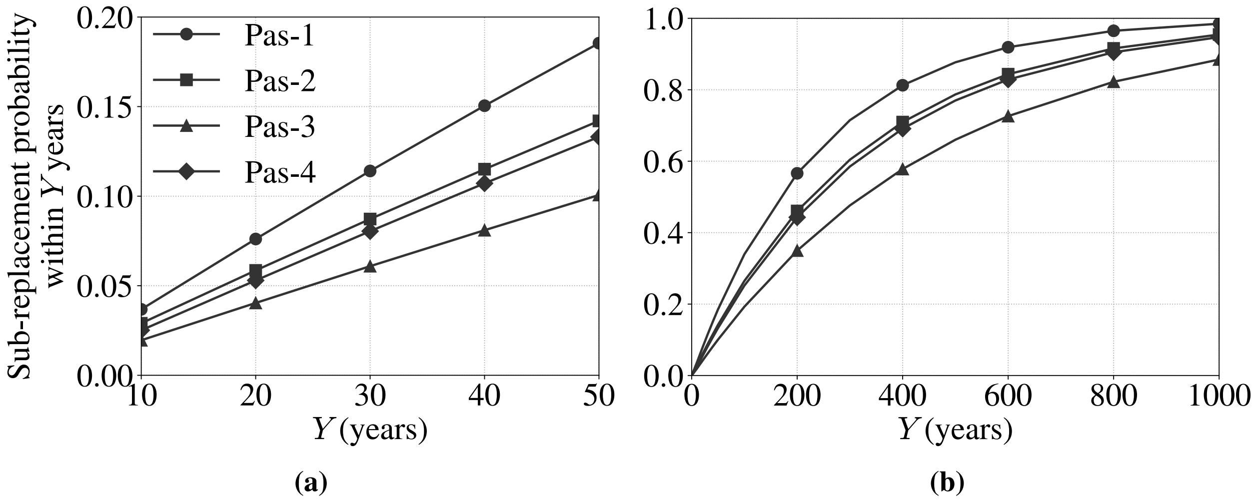

Fig. S-3. Probability of sub-replacement over time for four homes in Pascagoula. Panel (a) shows the probability of absorption within 10, 20, 30, 40, and 50 years. The relationship appears nearly linear because the stepwise probability of entering sub-replacement remains low and approximately constant. Panel (b) extends the time horizon to 1000 years, showing that cumulative probabilities converge to one, as expected.

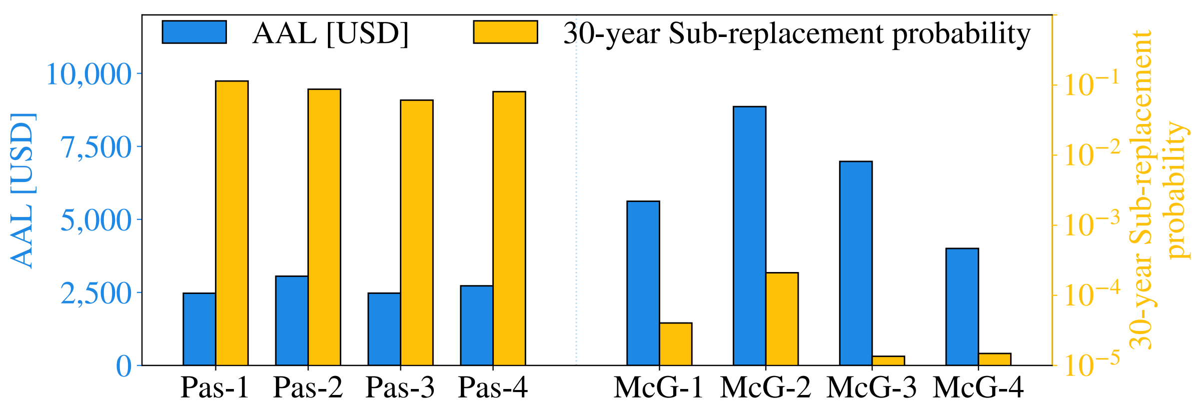

Fig. S-4. Annual Average Loss (left vertical axis) and 30-year sub-replacement probabilities (right vertical axis) for selected houses in Pascagoula and McGregor. Pascagoula houses are labeled *Pas-1* through *Pas-4*, and McGregor houses are labeled *McG-1* through *McG-4*. AAL is expressed in USD; sub-replacement probabilities are shown on a logarithmic scale.

price drop per flood event σ, and the clock parameter τ_0. These parameters introduce uncertainty because they depend on external factors such as economic conditions, homebuyer perceptions, and the availability of post-disaster funding. We estimated these parameters using available data and prior studies, but their true values remain uncertain, and it is therefore important to test how our results vary across plausible parameter ranges.

Using Pascagoula as a reference for topography and hazard characteristics, we generate a synthetic sample of houses. We consider a generic one-story single-family home and vary its flood exposure by adjusting ground elevation above NAVD88 (h_G) and FFHAG. Specifically, we vary h_G from 120 to 460 cm in 20 cm increments (18 levels), and assign FFHAG values from 20 to 240 cm, also in 20 cm increments (12 levels), resulting in 216 exposure combinations. For each combination, we assign four normalized base prices $\psi_0 \in \{0.50, 1.00, 1.50, 2.00\}$, resulting in a total of 864 houses. All houses share a single flood distribution, obtained by spatially averaging the probability density functions of the yearly maximum flood level H in Pascagoula.

For our sensitivity analysis, we first calculate sub-replacement probabilities for all houses using baseline parameter values ($R = 0.20$, $\sigma = 0.08$, $\tau_0 = 6$), and classify each house into five risk levels: Negligible ($< 10^{-4}$), Very Low (10^{-4}–10^{-3}), Low (10^{-3}–10^{-2}), High (10^{-2}–10^{-1}), and Very High (10^{-1}–1.00). We then vary one parameter at a time across five plausible values: $R \in \{1.00, 0.33, 0.20, 0.12, 0.10\}$, $\sigma \in \{0.04, 0.06, 0.08, 0.10, 0.12\}$, and $\tau_0 \in \{4, 6, 8, 10, 12\}$. Note that a higher value of r makes damaged houses more likely to be repaired every year, therefore reducing sub-replacement risk. In contrast, higher values of σ and τ_0 increase sub-replacement probability, since flood-related price drops are larger and take longer to recover.

Table S-3 shows the ranges of the median sub-replacement probabilities for different risk categories, obtained by varying each parameter independently. We observe two main trends. First, the model is relatively insensitive to changes in r and τ_0, while it is more sensitive to changes in σ. When either r or τ_0 is varied, median probabilities remain within the same order of magnitude. For example, when varying τ_0 from 4 to 12 years at $\psi_0 = 1.00$, the sub-replacement probability in the Very High risk category increases from 203 to 289‰—a relative change of 1.4×. In contrast, changing σ from 4‰ to 12‰ at the same ψ_0 level and risk category produces a much wider range: from 139 to 363‰—equivalent to a 2.6× change. The model is more sensitive to changes in σ because σ directly reduces the house price after each flood event, pushing the house closer to the sub-replacement threshold. In contrast, r and τ_0 influence the outcome indirectly by affecting the recovery duration.

Second, for increasing values of ψ_0, the sensitivity of the model to each parameter becomes more pronounced. While for $\psi_0 = 1.00$ the spread in median probability due to varying τ_0 was 86‰ (from 203 to 289‰), for $\psi_0 = 2.00$ the spread increases to 119‰ (from 79 to 198‰). The increase in sensitivity with higher ψ_0 is even more pronounced for σ. At $\psi_0 = 1.00$, the median probability for the Very-High risk sample ranges from 139 to 363‰ (a 2.6× difference). At $\psi_0 = 2.00$, it ranges from 0.8 to 384‰—an increase of nearly 480×. In conclusion, σ exerts the strongest influence on model outcomes, and sensitivity to parameter uncertainty increases with higher initial normalized base prices ψ_0.

REFERENCES

Atreya, A., Ferreira, S., and Kriesel, W. (2013). “Forgetting the Flood? An Analysis of the Flood Risk Discount over Time.” *Land Economics*, 89(4), 577–596 Publisher: University of Wisconsin Press Section: Articles.

Bin, O. and Landry, C. E. (2013). “Changes in implicit flood risk premiums: Empirical evidence from the housing market.” *Journal of Environmental Economics and Management*, 65(3), 361–376.

Bin, O. and Polasky, S. (2004). “Effects of Flood Hazards on Property Values: Evidence before and after Hurricane Floyd.” *Land Economics*, 80(4), 490–500 Publisher: [Board of Regents of the University of Wisconsin System, University of Wisconsin Press].

Ortega, F. and Taşpınar, S. (2018). “Rising sea levels and sinking property values: Hurricane Sandy and New York’s housing market.” *Journal of Urban Economics*, 106, 81–100.

TABLE S-3. Ranges of median sub-replacement probabilities (per thousand) across four risk categories, for different values of ψ_0 and each parameter varied independently: yearly repair rate r, price drop per flood event σ, and recovery clock parameter τ_0. Each range corresponds to the minimum and maximum median probability observed within the risk category when the parameter is varied across its full tested range, while all others are held constant. Probabilities lower than 10^{-4} are reported as 0, in accordance with the definition of the four considered risk levels.

Parameter {**range**}	ψ_0	**Very Low**	**Low**	**High**	**Very High**
r {1.00–0.10}	0.50	0.4–0.4	3.1–3.2	30–33	344–385
	1.00	0.2–0.3	2.6–3.2	28–38	212–266
	1.50	0.2–0.5	2.0–4.2	19–37	137–225
	2.00	0.2–0.5	2.3–5.8	18–40	107–197
σ {4%–12%}	0.50	0.3–0.6	2.3–4.6	23–43	276–430
	1.00	0–0.4	1.3–5.2	16–53	139–363
	1.50	0–2.6	0–15	1.2–100	28–383
	2.00	0–4.7	0–25	0–126	0.8–384
τ_0 {4–12}	0.50	0.4–0.4	3.1–3.4	30–36	338–402
	1.00	0.2–0.3	2.5–3.9	27–40	203–289
	1.50	0.1–0.9	1.3–6.5	15–47	116–248
	2.00	0–0.6	1.3–5.9	12–42	79–198